MICROSTRUCTURE-INFORMED SIMULATION OF STRAIN-REVERSAL TESTING SETUP FOR SHEET METAL FORMING

J. Gawad[1,2], P. Eyckens[3], D. Roose[1], A. Van Bael[3], P. Van Houtte[3]

[1]KU Leuven, Dept. Computer Science, Belgium
[2]AGH University of Science and Technology, Poland
[3]KU Leuven, Dept. Materials Engineering, Belgium

ABSTRACT: The Finite Element codes used in CAE typically neglect evolution of plastic anisotropy and exploit simplistic phenomenological hardening models. Such approach is unable to model complex hardening phenomena originating in the dislocation substructure of materials, such as cross-effect or Bauschinger effect. If a multi-operation sheet forming process is modelled, this may degrade accuracy of the predictions. To address this issue, we propose a hierarchical multi-scale plasticity framework, which takes into account combined texture evolution, anisotropy evolution and complex hardening. Owing to the multi-scale approach followed, the relevant phenomena are tackled at appropriate length scale by physics-based crystal plasticity models. We also propose a design of a test sheet forming process (Undulated Cup Bauschinger Test, UCBT) that allows studying complex strain path including strain reversal at high level of pre-deformation. The UCBT demonstrates how the concurrent evolutions of texture and substructure affect the plastic anisotropy and in turn the geometry of the deformed sample. It is found in this study that capturing the macroscopic effect of strain reversal requires both anisotropy evolution and dislocation-based hardening model combined, whereas the complex hardening alone may not be sufficient.

KEYWORDS: plastic anisotropy; multi-scale model; substructure; Bauschinger effect; sheet forming, plastic anisotropy, anisotropy evolution;

1 INTRODUCTION

It is widely recognized that crystallographic texture has a strong effect on anisotropic properties of polycrystalline metals. Another source of material anisotropy originates from the development of a complex and anisotropic dislocation patterning or grain substructure. The plastic deformation of metals involves complex interactions in the material microstructure, including evolution of the crystallographic texture and grain substructure. The effects of these interactions can be observed macroscopically, for instance as differential hardening, and as the Bauschinger effect. Nevertheless, simple isotropic hardening laws and yield locus models, which are commonly used in the Finite Element CAE generally fail to reproduce these effects. This limitation may lead to undesirable consequences in designing forming processes. If complex hardening becomes an important factor in a given forming process, a guidance from the FE CAE may result in either inappropriate choice of process parameters or in overly conservative process designs.
The sheet metal testing procedures usually do not incorporate studies on hardening phenomena that occur in the material at relatively high strains. A strain path change after a substantial pre-deformation is rarely investigated in industrial practice as well. This is partly because no standardized and uncomplicated test has been widely adopted to date.
This paper proposes a design of a test sheet forming process that allows one to study a complex strain path involving strain reversal at high level of pre-deformation. We also present how the concurrent evolution of texture and substructure affect the plastic anisotropy and as a consequence the geometry of the deformed part.

2 HIERARCHICAL MULTI-SCALE FRAMEWORK FOR POLYCRYSTAL PLASTICITY

This paper employs the hierarchical multi-scale approach to model the microstructural interactions that control the behavior of the material. The interactions are resolved by fine-scale models that act on relevant length scales, which are associated with the size of individual crystals and substructure inside crystals. As opposed to the embedded modelling, which

* Corresponding author: KU Leuven, Celestijnenlaan 200A, 3001 Heverlee, Belgium, tel: +32 16 327658, email: Jerzy.Gawad@cs.kuleuven.be

directly couples the fine-scale model inside a coarse-scale one, the hierarchical approach exploits approximations of the fine-scale models at the coarser length scale. From a computational point of view, the efficiency advantage of the hierarchical approach is attributed to the fact that the finer-scale material model is never *directly* invoked by the macroscopic material model to determine the homogenized material response. The hierarchical multi-scale (HMS) polycrystalline plasticity model [1] is extended in this paper to consider three distinct length scales:

1. macroscopic, which is suitable for simulating components or parts in sheet metal forming,
2. mesoscopic, which describes material at the level of crystal agglomerate comprising a few thousand grains,
3. microscopic, which resolves the contributions of different types of dislocations to the plastic slip on individual slip systems at the level of a single crystal.

The material description used in the elastic-plastic FE is derived from the Crystal Plasticity (CP) models by means of virtual experiments and subsequently approximated by appropriate analytical functions, as illustrated in Fig. 1. These functions are periodically reconstructed as needed, typically on condition that a pre-defined strain increment is reached or a substantial strain path change is detected.

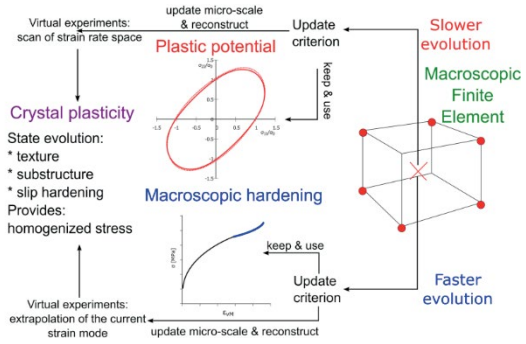

Fig. 1 *Overview of the hierarchical multi-scale framework for metal plasticity*

2.1 MACROSCOPIC MODEL

On the macroscopic scale, a continuum mechanics description of the material is followed, thus the Finite Element method can be adopted. The characteristic length scale corresponds to the size of a finite element in a simulation of metal forming, which is typically of the order of 1 mm. The properties are assumed to be homogeneous on this length scale, therefore all microstructural heterogeneities from the finer scales may be discarded.

In the presented scheme all plastic properties are derived from the finer-scale model by means of virtual experiments, but the computational procedure to determine a given effective property depends on its evolution rate. It is crucial to notice that in many metallic alloys the plastic anisotropy evolves less rapidly than the yield stress of the material. The plastic anisotropy is primarily modelled by means of the yield locus concept. The shape of the yield locus is given by the Facet plastic potential [2], which is adaptively reconstructed with increasing plastic strain. However, the shape of the yield locus is assumed to be constant between the consecutive reconstructions. For the details of the reconstruction procedure, the reader is referred to [1]. On the other hand, the evolution of the yield locus size, or in other words the hardening, develops much faster, thus the assumption of constant property cannot be justified in this case. The hierarchical framework tackles the evolution of the yield locus size by calculating a piece-wise hardening function, which is incrementally recalibrated along the recent deformation path.

It is worth mentioning that the updates of the yield locus shape and size are conducted independently. Prior to any update, the evolution of internal variables in the finer-scale models is calculated.

2.2 MESOSCOPIC CRYSTAL PLASTICITY MODEL

The mesoscopic length scale model deals with aggregates of individual grains. The typical dimension of crystals is in the micrometer range. Each grain has a crystal lattice orientation, and associated slip systems that accommodate the plastic deformation. The initial crystal orientations are selected in such a way that the aggregate as a whole approximates the texture of the material determined from measurement. For statistical reasons, a few thousand crystals are included in the virtual polycrystalline aggregate. The crystal rotations, as well as the slips on the available deformation systems, are predicted by the ALAMEL crystal plasticity model [3]. The critical resolved shear stresses (CRSS) needed by the ALAMEL model are calculated by the substructure model presented below. The ALAMEL model also delivers the homogenized stress response to the superimposed plastic strain or strain rate, which is needed for calibrating the plastic properties at the coarser length scale.

2.3 SUBSTRUCTURE EVOLUTION MODEL

The microscopic scale model resolves the dislocation substructure, which typically has sub-micron dimensions. The anisotropic substructure model [4] is adopted here. The model postulates a number of dislocation density evolution equations on the scale of the grain substructure, based on physical principles and also supported by experimental TEM observations [5]. Three distinct types of immobile dislocations are considered:

1. dislocations the boundaries of randomly-oriented cells (Cell Boundaries – CBs), which contribute to isotropic hardening,
2. dislocations contained within planar Cell Block Boundaries (CBBs), which develop

along the most active (110) crystallographic planes causing latent hardening, and

3. polarized dislocations at CBBs, which are directionally mobile. The re-mobilization of the polarized dislocations lowers the flow stress upon slip reversal.

Contributions from these types of dislocation densities are combined to derive the CRSS for each individual slip system within each particular crystal. In the event of a strain path change, the active slip systems drastically change. This immediately affects the local stresses, and the stress homogenized over the crystal aggregate. With ongoing deformation after strain path change, the substructure is drastically changed, including destruction of old CBBs and replacement with more favorably-oriented CBBs. Also the crystal rotations evolve differently as before the strain path change.

A macroscopic effect of the change to the substructure is visible as transient hardening, for instance cross effects and Bauschinger effect. Cross effects arise due to replacement of the old dislocation structure by a new one that is more accommodated to the loading conditions. The Bauschinger effect can also be captured, since the polarized (directionally-mobile) dislocation densities partially destroy the substructure upon reversal of the strain path.

3 UNDULATED CUP BAUSCHINGER TEST

The complex hardening phenomena tend to occur in sheet forming processes, in particular multi-stage that involve a sequence of operations. However, mechanical tests are rarely capable of delivering appropriate material characterization. A test that would measure complex hardening should allow one to (1) study a considerable strain path change, such as the strain reversal, and (2) do so at relatively high strain level, since this is typically the operational regime of sheet metal forming, and (3) involve no additional steps, such as cutting out samples from a deformed part followed by flattening, which may introduce additional deformation and distort results of the experiment.

In this paper we propose a testing procedure that satisfies the requirements given above. It includes strain path reversal at high strain level, implemented in two consecutive forming operations on the same part. The Undulated Cup Bauschinger Test (UCBT) comprises two consecutive forming operations. The first one is a basic deep drawing of axisymmetric cups. In the second operation, which is called grooving, the punch tool is replaced with a grooved die, and the cup wall is deformed by side punches that move radially towards the center of the cup.

Whereas during the first operation the flange area is subjected to circumferential compression, the second forming step introduces tensile deformation along the circumferential direction in the cup wall zone. The UCBT process allows substantial reversal of the strain path (e.g. strain increment of $\varepsilon_{vM} \approx 0.4$ can be imposed in the second step) at relatively high pre-strains (e.g. $\varepsilon_{vM} \approx 0.7$) reached at the end of the first stage. In many materials these deformation conditions may trigger the Bauschinger effect within the cup wall area.

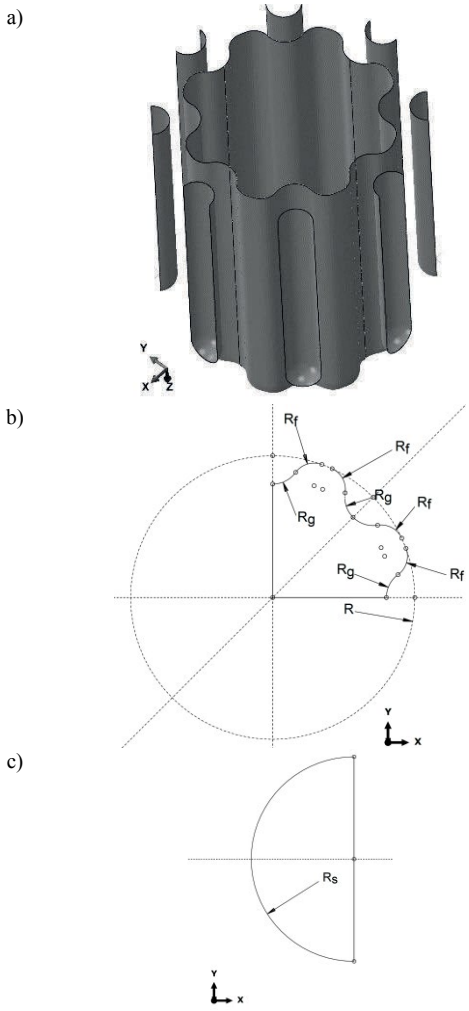

Fig. 2 *Toolset used in the grooving operation: a) 3D view of the assembly consisting of the grooved die and 8 side punches, b) x-y section of the grooved die, c) x-y section of the side punch*

Below we summarize the design details of the testing setup. The dimension of cup drawing dies are as follows: diameter of the punch: 50 mm, punch fillet radius: 7 mm, die diameter: 52 mm and die fillet radius: 6 mm. The toolset used in the grooving step is presented in Fig. 2. The following dimensions of the toolset are used: R = 25mm, R_g = 5 mm, R_f = 4 mm and R_s = 4 mm.

In this paper we employ the setup that includes 8 side-punches, which are radially positioned at 45° with respect to each other. Simpler variants of the setup exist that contain either 2 or 4 side-punches positioned every 180° or 90°, respectively.

4 RESULTS AND DISCUSSION

The Abaqus/Explicit FE code is used to solve the macroscopic deformation problem. The multi-scale HMS framework is incorporated as VUMAT user material subroutine.

The material used in the study is a 0.7 mm thick sheet of batch-annealed IF deep drawing DC06 steel. A circular blank of diameter 100 mm is subjected to the first forming operation. One quarter of the blank is modelled, exploiting the symmetry properties of the blank and the process. About 15 000 8-node continuum elements with reduced integration (C3D8R) are used to discretize the blank. Whereas this study makes use of continuum elements, the HMS can also be exploited with shell or continuum shell elements. Each integration point holds internal state variables of the fine-scale model. These include 5 000 crystals, each containing the state variables representing the dislocation densities of the substructure. The multi-scale model of the whole blank thus comprises approximately 75 million crystals.

We present a series of numerical experiments assuming different contributions to the plastic anisotropy evolution. The following cases are considered where the anisotropy evolution results from:

Case A. texture evolution in combination with the substructure evolution (CBs, CBBs and polarized dislocations at CBBs included),

Case B. texture evolution in combination with evolution of CB and CBB dislocation types,

Case C. texture evolution combined with CB dislocation evolution,

Case D. texture evolution in combination with substructure evolution (CBs, CBBs and polarized dislocations at CBBs included), however the plastic potential is not updated and kept constant throughout the process.

The cases A – C include evolution of plastic potential, whereas the last case takes account of just the complex hardening of the material derived from the mesoscopic and microscopic level.

Case A takes into account the polarized dislocations at CBBs that remobilize on strain path reversal. It can be then expected that the grooving operation shall reduce the density of the polarized dislocations. This effect is accompanied with transient decrease in flow stress, even though the strain increases. In contrast, case B does not consider polarized dislocation densities, while the CBBs with related latent hardening aspect are included. The case C is a further simplification, in which the substructure is approximated by a single dislocation density representing randomly-oriented CBs. This case is essentially identical to the Kocks-Mecking strain hardening model [6].

As seen in Fig. 3, the zones in the sample where the density of polarized dislocations decrease generally coincide with the regions deformed by the grooving operation. It can also be noticed that in the zones under the side punches the density of polarized dislocations commence to re-develop, however only on the side of the cup interior, since it is subjected to more monotonic loading.

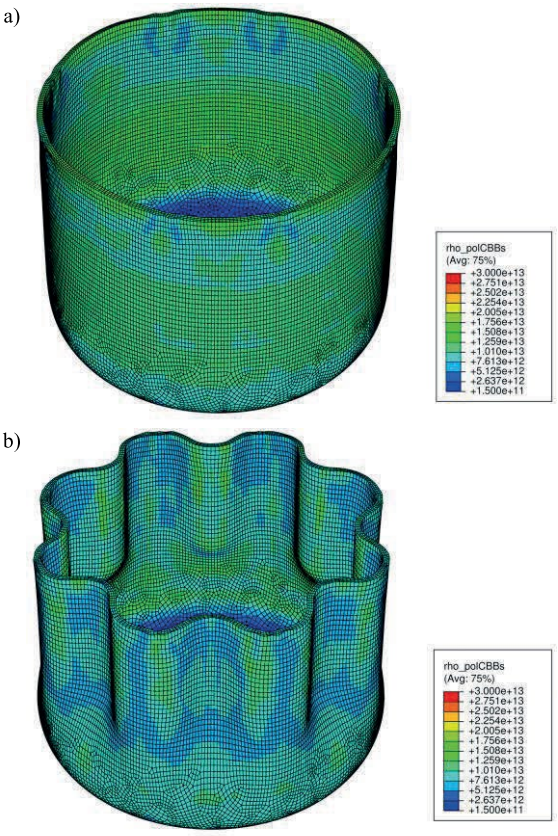

Fig. 3 *Density of polarized dislocations superimposed on the deformed mesh (Case A): a) after cup drawing, b) after grooving*

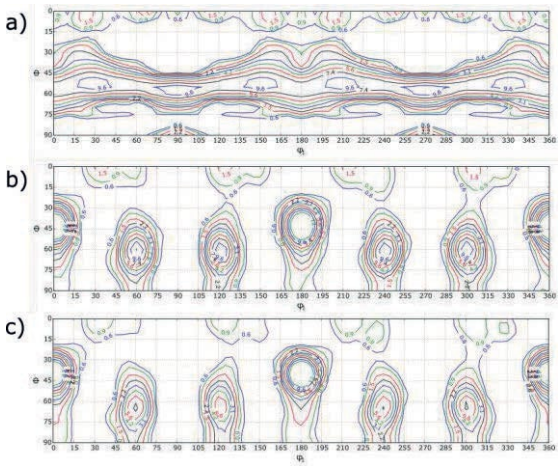

Fig. 4 *Texture evolution at the material point located approx. 5 mm from the verge of the blank at the RD in Case A. φ_2=45° section of the ODF is shown for: a) initial texture (TI=4.0), b) deformation texture after the cup drawing (TI=5.68), c) deformation texture after the grooving operation (TI=5.8)*

Although the HMS model keeps track of the anisotropy evolution in the entire deformable FE mesh, for sake of simplicity we limit the presentation of the per-point results to one element, which is located approximately 5 mm from the rim of the blank at RD. Texture evolution in this element is presented in Fig. 4. The φ_2=45° sections of the orientation distribution function (ODF) are shown along with the texture index (TI) that characterizes the global sharpness of texture. As can be seen, the γ-fiber, which dominates in the initial texture, breaks down into new texture features. The decomposition of the γ-fiber during the cup drawing operation is accompanied with intensification of texture. Although the strain reversal during the grooving considerably diminishes some of the new components, the overall texture intensity is modified only to limited extent.

Fig. 5 shows how the yield locus evolves in cases A–C in the considered material point. The most remarkable influence on the yield locus shape is consistently found in the first and third quadrants of the presented yield locus sections. This is despite the fact that the cup drawing operation imposes a stress state that is characterized by the stress ratio σ_{11}/σ_{22} varying approximately in the range of (-0.1,-0.6) and thus in the fourth quadrant of the yield locus sections shown in Fig. 5. The corresponding yield locus zone is hardly affected, which indicates occurrence of a cross effect. This also takes place if the Kocks-Mecking approach (Case C) is followed (Fig. 5c). Since this is essentially an isotropic hardening model, the observed effect most likely originates in the texture evolution. Another notable regularity that appears in Fig. 5 is that the yield locus after the grooving step is generally similar in all the considered cases, albeit substantially different from the initial one. On the other hand, the shape of the yield locus at the end of the intermediate cup drawing operation largely depends on the substuctural contributions included in the model. If Case C is considered, the grooving operation does not remarkably alter the shape of the yield locus, even though the texture at this location changes. If the dislocations contained within the CBBs are taken into account (Case B, cf. Fig. 5b), the evolution of the yield locus during the cup drawing appears less pronounced, but the cross effect magnifies. This also holds, admittedly to smaller extent, in the model that also considers the polarized dislocations at CBBs (Case A).

The macroscopic effect of different contributions to the evolution of plastic anisotropy can be seen in Fig. 6. One may distinct two groups in the results presented there. The first group comprises the cases in which the substructure does not affect yield locus shape, comprising of Case D (the shape of the yield locus is kept constant and complex hardening is used) and of Case C (the Kocks-Mecking hardening does not affect the yield locus shape but the texture evolution does. The cup profiles in these two cases generally coincide at the end of both forming operations. Moreover, they are insensitive to strain reversal introduced by the grooving step. The second group includes Case A and B, for which inclusion of an anisotropic substructure does affect yield locus shape. The distinctive feature compared to the first group is that the predicted cup profiles have much less pronounced ears that lack a clear minimum at 45° w.r.t. the RD. The origin of this difference with respect to the first group is believed to be found in the strain path changes that occur during the draw-in through the superimposed sheet bending and unbending over the die radius.

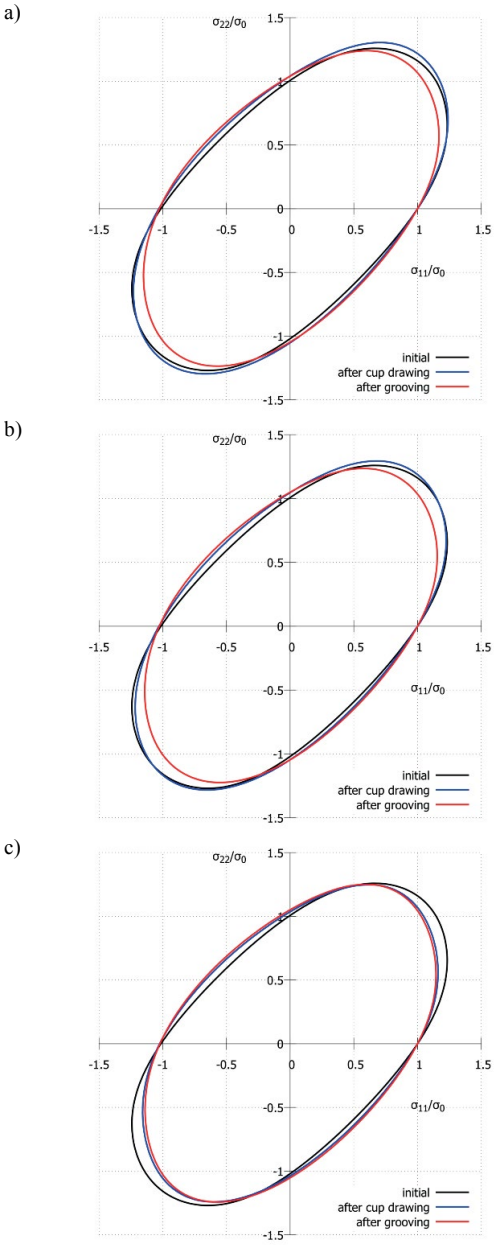

Fig. 5 *Evolution of the yield locus obtained in the cup drawing and the grooving operation, depending on the types of dislocations taken into account: a) CB, CBB and polarized dislocations (Case A), b) CB and CBB (Case B), and c) CB (Case C)*

The effect of strain reversal during the grooving operation is undoubtedly visible in Case A, which takes into account the polarized dislocations at CBB. The remobilization of the dislocations softens the material, which results in generally lower cup height at the end of the grooving operation, since the material can more easily deform. This leads us to the conclusion that in the simulated UCBT process the Bauschinger effect is fully captured only if (1) texture evolution is considered, (2) the plastic potential evolves and (3) a sufficiently rich hardening model is used.

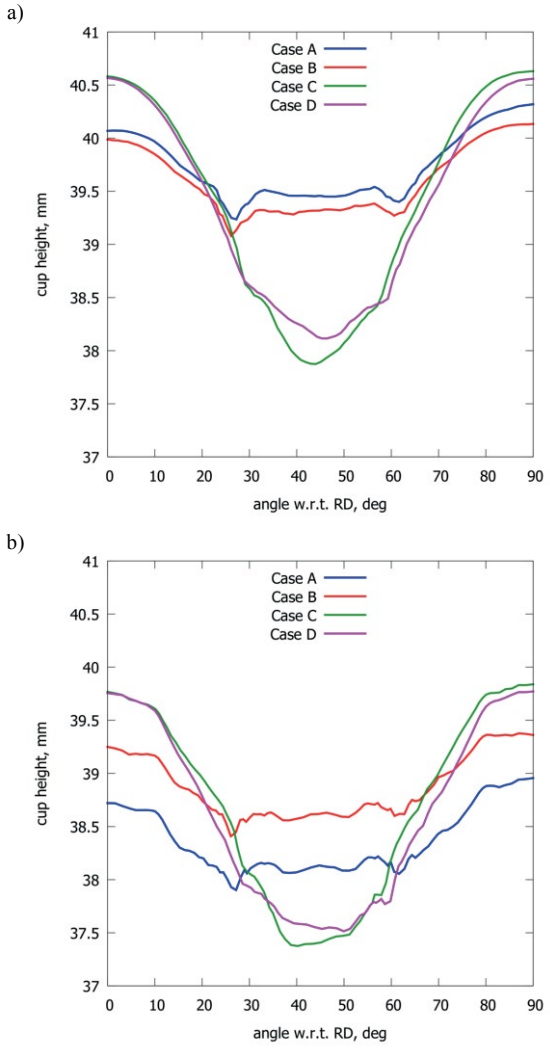

Fig. 6 *Cup profile at the end of the (a) cup drawing and (b) grooving operations.*

5 CONCLUSIONS

The presented hierarchical multi-scale model allows one to capture the combined effects of texture and substructure evolution in sheet metal forming simulations. Although the final evolved yield locus was found much similar regardless of considered contributions to anisotropy evolution, the intermediate yield loci were remarkably affected. This may be of importance to accuracy in simulating forming processes that consist of multiple consecutive operations. The presented results suggest that hardening model alone, even though it is based on evolution of texture and considers complex interactions in the substructural features at the level of individual slip systems, may not be sufficient to predict the effect of strain reversal.

6 ACKNOWLEDGEMENT

The authors gratefully acknowledge the financial support from the Knowledge Platform M2Form, funded by the Industrial Research Fund KU Leuven. The computational resources and services used in this work were provided by the VSC (Flemish Supercomputer Center), funded by the Hercules Foundation and the Flemish Government.

REFERENCES

[1] Gawad, J., Van Bael, A., Eyckens, P., Samaey, G., Van Houtte, P., Roose, D.: *Hierarchical multi-scale modeling of texture induced plastic anisotropy in sheet forming.* Computational Materials Science, 66:65–83 2013.

[2] Van Houtte, P., Yerra, S. K., Van Bael, A.: *The Facet method: A hierarchical multilevel modelling scheme for anisotropic convex plastic potentials.* International Journal of Plasticity, 25(2):332–360 2009.

[3] Van Houtte, P., Li, S., Seefeldt, M., Delannay, L.: *Deformation texture prediction: from the Taylor model to the advanced Lamel model.* International Journal of Plasticity, 21(3): 589–624 2005.

[4] Peeters, B., Seefeldt M., Teodosiu C., Kalidindi S.R., Van Houtte P., Aernoudt E., *Work-hardening/softening behaviour of b.c.c. polycrystals during changing strain paths: I. An integrated model based on substructure and texture evolution, and its prediction of the stress-strain behaviour of an IF steel during two-stage strain paths*. Acta Materialia,. 49(9): 1607-1619 2001

[5] Peeters, B., Bacroix B., Teodosiu C., Van Houtte P., Aernoudt E., Work-*hardening/softening behaviour of b.c.c. polycrystals during changing strain: : Part II. TEM observations of dislocation sheets in an IF steel during two-stage strain paths and their representation in terms of dislocation densities*. Acta Materialia, 49(9):1621-1632 2001

[6] Mecking, H., Kocks, U.: *Kinetics of flow and strain-hardening*. Acta Metallurgica 29, 1865-1875 1981.